Growth laws for the phase ordering dynamics of the *B*1 phase of a bent-core liquid crystal

HoKei Chan and Ingo Dierking*
Department of Physics and Astronomy, University of Manchester, Schuster Laboratory, Oxford Road, Manchester M13 9PL, United Kingdom
(Received 3 March 2004; published 30 August 2004)

We have experimentally investigated the dynamics of the phase ordering process of bent-core molecules at isothermal conditions, forming the liquid crystalline "banana" *B*1 phase from the isotropic melt. In contrast to the fractal growth patterns observed for other "banana" liquid crystal phases, the *B*1 phase exhibits dendritic-like growth, which at short times shows similar growth structures as observed for conventional smectic bâtonnet growth. Analysis with respect to growth laws of the form $L(t) \sim t^n$ shows that the growth process follows the theoretically predicted Allen-Cahn dynamics with $n=1/2$ for zero difference in the free energy between the high- and the low-temperature phase, while the growth exponent approaches $n \rightarrow 1$ for increasing supercooling. From the experimentally obtained data, we estimate the ratio between volume and curvature driven contributions to the phase ordering process as a function of supercooling and suggest a phenomenologically determined relationship of $\log \Delta F \sim \Delta T$ for the difference in free energy between the high- and the low-temperature phase as the quench depth is varied.

DOI: 10.1103/PhysRevE.70.021703 PACS number(s): 61.30.−v, 64.70.Md, 64.60.Qb, 68.70.+w

I. INTRODUCTION

Phase ordering processes after a quench, i.e., the rapid change of an intensive thermodynamic variable of state, are of fundamental importance for the processing of materials, ranging from metal alloys and glasses to polymers, all the way to the crystallization of pharmaceutical organic compounds [1]. In a temperature quench experiment, the temperature T of a system is rapidly decreased across a phase transition (at constant pressure) from a region of the phase diagram, where the system is uniform in its high-temperature phase, into a metastable region, where the low-temperature phase is thermodynamically favored. Thermal fluctuations induce nucleation of the low-temperature phase and germs grow spontaneously once a critical nucleus size is exceeded. This size is very small and cannot be observed by optical techniques. The subsequent growth process can be described by a characteristic length L, which is dependent on time, i.e., $L(t)$. At times, when nucleus growth can be followed optically, the time evolution of the characteristic length L can be described by a growth law,

$$L(t) \sim t^n, \tag{1}$$

where n is called the growth exponent. The value of the growth exponent n depends on the universality class, as classified by Hohenberg and Halperin [2]. Liquid crystals fall into the category of "model *A*" dynamics [3] [nonconserved order parameter (NCOP)], as a temperature quench induces a phase transition between the isotropic phase with order parameter $S=0$ to a partially ordered liquid-crystal phase with $0<S<1$. During the isothermal phase ordering process after the temperature quench, we have a nonequilibrium situation with the low-temperature liquid crystal phase ($S \neq 0$) growing in the "sea" of the high-temperature isotropic phase ($S=0$). During growth, the isotropic and the liquid crystal phase are separated by a sharp domain boundary and the velocity of the local domain interface is equal to the local curvature of the germ. The change of the characteristic length L with time can be described as

$$\frac{dL(t)}{dt} = C\frac{1}{L(t)} \tag{2}$$

with C being a constant. Integration gives a growth exponent of $n=1/2$, thus

$$L(t) \sim t^{1/2}, \tag{3}$$

which is independent of the spatial dimension of the sample. This general result was already obtained by Lifshitz [4] and by Allen and Cahn [5], the latter also giving experimental evidence for the case of metal alloys. Other investigations on solid-state materials followed [6,7]. Direct confirmation of Eq. (3) by numerical methods was presented by several authors [8–11] and recently in a large-scale computation by Brown and Rikvold [12].

It is worthwhile to note that the above growth law [Eq. (3)] not only holds for spherical but also for elliptical germs. In the latter case, $L(t)$ depends on direction. A suitable characteristic length to investigate experimentally in the case of elliptical germs is the long and/or the short axis of the ellipse. It can be shown from the definition of the local curvature that shape invariance, i.e., a constant ratio between the long and the short axis of an ellipse, leads to the same growth law [Eq. (3)] for both characteristic lengths. And indeed, the growth exponents for both of these characteristic lengths are in first approximation equal, as has been demonstrated experimentally for the anisotropic bâtonnet growth of a Sm*A* liquid crystal [13].

*Author to whom correspondence should be sent. Email address: dierking@reynolds.ph.man.ac.uk

It has been pointed out by Bray [14] that the $t^{1/2}$ growth law is only valid for pure curvature driven growth at zero difference in the free energy, $\Delta F=0$, i.e., for quench depth $\Delta T=0$. For increasing quench depth, ΔF is different for the low- and the high-temperature phase and a volume driving term cannot be neglected. Following the discussion in Ref. [15], Eq. (2) has to be extended to

$$\frac{dL(t)}{dt} = C\frac{1}{L(t)} + V, \tag{4}$$

where V is a constant proportional to ΔF, the latter in turn being a function of quench depth, i.e., $V=V[\Delta F(\Delta T)]$. Separation of variables and integration by substitution gave the final result,

$$\frac{L(t)}{V} + \frac{C}{V^2}\ln\left(\frac{C}{C+VL(t)}\right) = t. \tag{5}$$

Equation (5) cannot be brought into the form of a growth law analogous to Eq. (3). However, by assuming a reasonable value of C and different values for V, $L(t)$ data can be generated computationally from Eq. (5), which then provides different growth exponents n as the ratio V/C, i.e., the ratio between volume driven and curvature driven growth contributions, is varied. Comparison with the experimentally determined growth exponents thus allows a discussion of the relative influences of curvature versus volume driven growth.

Surprisingly, only a few reports have been published on the growth of liquid crystals, despite the fact that their isothermal phase ordering process can easily be followed by polarization microscopy and digital image analysis, due to the optical anisotropy of liquid crystals. Reports include the recent studies on frustrated blue phases [16], nematic and smectic phases [15], more detailed investigations of cholesteric materials [17,18], and the anisotropic growth of smectic bâtonnets [13].

The novel "banana" phases, comprised of bent-core mesogens, have recently attracted much attention with respect to chiral phase properties from achiral molecules [19]. In contrast to the phase ordering of conventional thermotropic phases, the "banana" phases often exhibit fractal growth structures [20–22]. An exception is found in the $B1$ phase. Initial growth of liquid crystalline germs is very similar to that of conventional smectic bâtonnets. Once these germs have grown to come into close proximity of each other, dendritic-like growth patterns develop as depicted in Fig. 1, the textures being similar to those observed for discotic liquid crystals. At even later times, these dendritic structures coarsen to form a mosaic texture [23]. It is the isothermal growth at short times in the bâtonnet regime of the "banana" $B1$ phase that is the topic of this study.

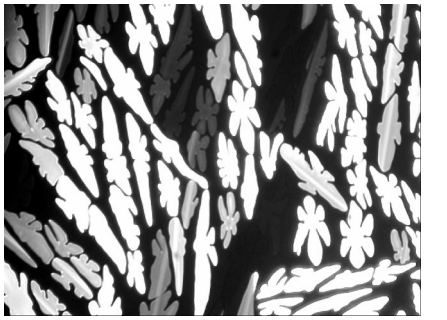

FIG. 1. Typical polarizing microscopic texture of the liquid crystalline "banana" $B1$ phase, showing clear features of dendritic growth. The image size is 520 μm $\times$ 390 μm.

II. EXPERIMENT

The compound investigated has the following structural formula:

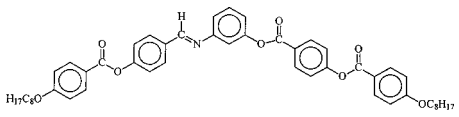

Its phase sequence, as determined by polarizing microscopy on cooling, is given by Iso. 124 B1 110 Cr.

The material was filled into commercially available sandwich cells (E.H.C., Japan) of cell gap $d=2$ μm by capillary action in the isotropic phase. The growth of the $B1$ phase was followed at isothermal conditions after a temperature quench by time-resolved digital image acquisition (JVC model KY-F1030U) in polarizing microscopy (Nikon Optiphot-Pol), equipped with a Linkam TMS91 hot stage for control of relative temperatures to better than 0.1 K. Digital images were recorded at a resolution of 1280×960 pixels, corresponding to an image size of 520 μm $\times$ 390 μm, for further analysis by software IMAGETOOL 3.0, developed at the University of Texas Health Science Center, San Antonio. Samples were quenched from the isotropic phase at a rate of 3 K min^{-1}, which represented the best compromise between electronic temperature regulation and achievable quench depth. The quench depth was varied from $\Delta T=0.0$ K ($\Delta F=0$) to $\Delta T=0.7$ K ($\Delta F\gg0$). For larger quench depths, nucleation commenced before the final temperature was reached, i.e., growth could not be followed under isothermal conditions.

III. EXPERIMENTAL RESULTS AND DISCUSSION

Figure 2 depicts a typical time series of isothermal growth images of the $B1$ phase (bright) from the isotropic melt (black) at a quench depth of $\Delta T=0.3$ K (only selected images are shown; the actual frame rate was one image every 2 s, taken over a time period of more than 1 min). Nuclei grow in an anisotropic fashion, although without a preferred direction, somewhat similar to the bâtonnet formation of smectic liquid crystals [13], and can in a good approximation be treated as ellipses. Dendritic growth patterns develop at later times, most pronouncedly observed after the growth of the long bâtonnet axis is hindered by the growth of other

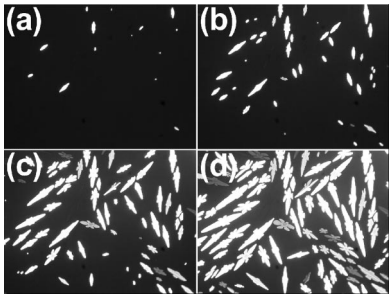

FIG. 2. Exemplary time series of polarizing microscopic growth images of the $B1$ phase at a quench depth of $\Delta T=0.3$ K and isothermal conditions after a temperature quench across the isotropic (black) to the liquid crystalline $B1$ phase (bright): (a) $t=8$ s, (b) $t=12$ s, (c) $t=16$ s, and (d) $t=20$ s. The individual image size is 520 μm$\times$390 μm. At early times, growth proceeds via bâtonnets, while at later times dendritic growth is observed.

germs. In this investigation, we exclusively study the growth of bâtonnet-like germs, before a dendritic structure starts to develop. The time regime of our investigations is thus limited by two factors: (i) the quench depth ΔT, because larger quench depths imply faster growth, and (ii) the distance with respect to other formed germs, which nucleate at arbitrary sites. Considering the latter factor, we only chose germs that were most isolated, in order to be able to follow their growth over as long a time period as possible. In all cases, care was taken to only study germs that were undisturbed by neighboring growing nuclei. Thus, as the characteristic length $L(t)$ we determined the length of the long axis of a growing germ in the time regime where it is undisturbed by other growing nuclei. From analysis of various image series, the experimental growth data $L(t)$ were obtained, some of which are illustratively shown in Fig. 3 for several quench depths as indicated in the figure legend. These data are used for the determination of the growth exponent n. At later times, the different nuclei approach each other and growth slowly ceases, leading to $L(t)=$const on contact. The latter time regime can clearly be identified by a change of slope in the log-log representation of $L(t)$ versus t used for the determination of the growth exponents, deviating in the linear scaling behavior. These data were obviously disregarded in the present analysis, as they do not represent uninfluenced nucleus growth.

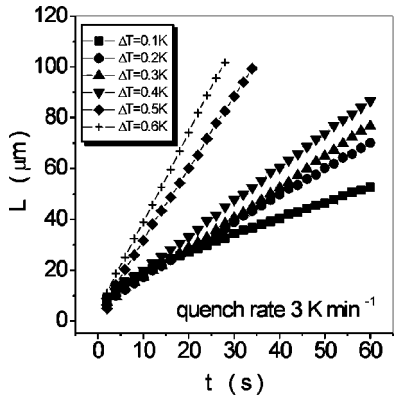

FIG. 3. Experimentally determined growth data $L(t)$ for a variety of different quench depths, as indicated in the legend of the graph. The characteristic length is taken as the long axis of growing nuclei.

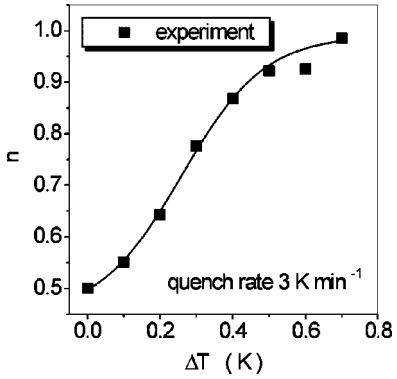

FIG. 4. Experimentally determined growth exponent n as a function of quench depth ΔT. Errors are in the order of the size of the symbols. The data confirm the theoretically predicted change of $n=1/2$ for $\Delta T=0$ K to $n\rightarrow 1$ for large quench depths.

Figure 4 shows the obtained growth exponents n as a function of quench depth ΔT (the solid line is a guide to the eye). For very small quench depths in the vicinity of the transition from isotropic to $B1$, i.e., at vanishing difference of the free energy $\Delta F\sim 0$ between the two phases, a growth exponent of approximately $n=1/2$ was obtained, in accordance with theoretical predictions by Lifshitz [4] and Allen and Cahn [5]. At larger quench depths, i.e., $\Delta F\gg 0$, the growth exponent approaches values of $n\rightarrow 1$. This behavior is in accordance with theoretical predictions [14], as well as with experimental trends first discussed for nematic liquid crystals [15]. By use of Eq. (5), $L(t)$ growth data can be generated numerically for different ratios of the volume driving term V to the curvature driven term C, where $C=1.5\times 10^{-13}$ m^2 s^{-1} was chosen to obtain growth data comparable to those observed in the experiments. From these data, we can subsequently determine growth exponents n as a function of V/C, as depicted in Fig. 5. Note that these are given

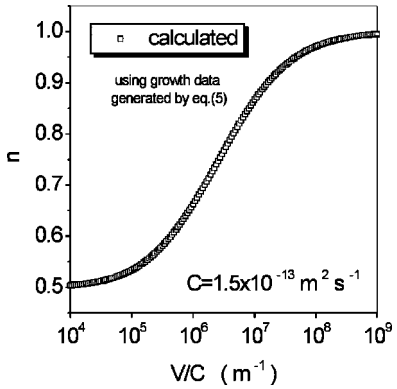

FIG. 5. Growth exponent n as a function of the ratio between the volume driving term V and the curvature driving term C. V/C is given in SI units with $C=1.5\times 10^{-13}$ m^2 s^{-1} to obtain data similar to that of the experiments. The growth exponent n is determined from numerically generated $L(t)$ data according to Eq. (5).

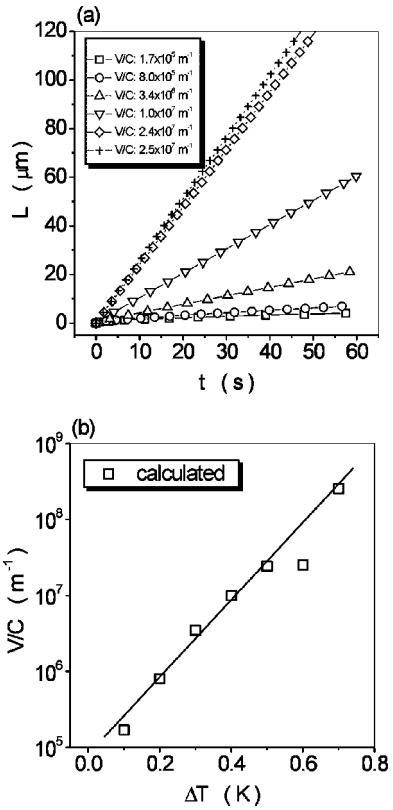

FIG. 6. (a) Numerically generated growth data $L(t)$ [Eq. (5)] with $C=1.5\times10^{-13}$ m^2 s^{-1}, which resembles the experimentally obtained growth curves depicted in Fig. 3. (b) Ratio between volume and curvature driven growth contributions as a function of quench depth ΔT, determined numerically for the experimental data relating to Fig. 4. The analysis suggests a phenomenological relationship of $\log \Delta F \sim \Delta T$ for the quench depth dependence of the difference in free energy between the high- and the low-temperature phase for increasing supercooling.

in SI units, not in arbitrary units like in an earlier study [15], and that the behavior of $n(V/C)$ exhibits the same qualitative functionality as the experimentally determined $n(\Delta T)$ curve (Fig. 4), when plotting V/C on a logarithmic scale. We also point out that our obtained results are in qualitative accordance with the previous calculations in arbitrary units, if we would set $C=1$. Determining n from $L(t)$ as a function of the ratio of the volume to curvature term, we can estimate V/C for the actual experimentally determined growth exponents through iteration. The corresponding data of the characteristic length L as a function of time t are shown in Fig. 6(a), while the determined ratios V/C are depicted as a function of quench depth in Fig. 6(b). The latter plot suggests that the logarithm of the ratio between the volume to curvature driving term, $\log(V/C)$, increases linearly with quench depth ΔT. As $V\sim\Delta F$ and $C=$const, this implies that the logarithm of the difference in free energy ΔF between the high- and the low-temperature phase is proportional to the quench depth,

$$\log \Delta F \sim \Delta T. \tag{6}$$

Equation (6) phenomenologically relates the change of free energy to the degree of supercooling the liquid crystal's low-temperature phase from the high-temperature isotropic phase.

IV. SUMMARY AND CONCLUSIONS

An experimental investigation of the phase ordering process of the "banana" $B1$ phase of bent-core liquid crystals has shown that growth mainly proceeds in a smectic bâtonnet-like fashion at short times, while developing into dendritic growth at later time scales. An analysis in terms of growth laws confirms the theoretically predicted behavior of a changing growth exponent from $n=1/2$ for zero quench depth to $n=1$ for large supercooling. The experimental results were discussed in terms of curvature driven versus volume driven growth, and it was shown that the volume term strongly dominates over the curvature term for increasing quench depth.

ACKNOWLEDGMENTS

We would like to thank W. Weissflog for generously providing the liquid crystal material studied in this investigation. Financial support from The Nuffield Foundation under Grant No. NAL/00680/G is also gratefully acknowledged.

[1] L. Ratke and P. W. Voorhees, *Growth and Coarsening* (Springer, Berlin, 2002).
[2] P. C. Hohenberg and B. I. Halperin, Rev. Mod. Phys. **49**, 435 (1977).
[3] P. M. Chaikin and T. C. Lubensky, *Principles of Condensed Matter Physics* (Cambridge University Press, Cambridge, 1995).
[4] I. M. Lifshitz, Sov. Phys. JETP **15**, 939 (1962).
[5] S. M. Allen and J. W. Cahn, Acta Metall. **27**, 1085 (1979).
[6] B. Park, G. B. Stephenson, S. M. Allen, and K. F. Ludwig, Phys. Rev. Lett. **68**, 1742 (1992).
[7] R. F. Shannon, S. E. Nagler, C. R. Harkless, and R. M. Nicklow, Phys. Rev. B **46**, 40 (1992).
[8] O. G. Mouritsen and E. Praestgaard, Phys. Rev. B **38**, 2703 (1988).
[9] F. Corberi, A. Coniglio, and M. Zannetti, Phys. Rev. E **51**, 5469 (1995).
[10] M. Fialkowski, A. Aksimentiev, and R. Holyst, Phys. Rev. Lett. **86**, 240 (2001).
[11] S. J. Mitchell, G. Brown, and P. A. Rikvold, Surf. Sci. **471**, 125 (2001).
[12] G. Brown and P. A. Rikvold, Phys. Rev. E **65**, 036137 (2002).
[13] I. Dierking and C. Russell, Physica B **325**, 281 (2003).
[14] A. J. Bray, Adv. Phys. **43**, 357 (1994).
[15] K. Dieckmann, M. Schumacher, and H. Stegemeyer, Liq. Cryst. **25**, 349 (1998).

[16] E. Demikhov, H. Stegemeyer, and T. Blümel, Phys. Rev. E **49**, R4787 (1994).
[17] I. Dierking, J. Phys. Chem. B **104**, 10 642 (2000).
[18] I. Dierking, Appl. Phys. A: Mater. Sci. Process. **72**, 307 (2001).
[19] For an overview of bent-core molecules and their "banana phases," see G. Pelzl, S. Diele, and W. Weissflog, Adv. Mater. (Weinheim, Ger.) **11**, 707 (1999), and references therein.
[20] I. Dierking, ChemPhysChem **2**, 59 (2001).
[21] I. Dierking, J. Phys.: Condens. Matter **13**, 1353 (2001).
[22] I. Dierking, H. Sawade, and G. Heppke, Liq. Cryst. **28**, 1767 (2001).
[23] I. Dierking, *Textures of Liquid Crystals* (Wiley-VCH, Weinheim, 2003), see plates 109 A and 109 B.